Different iron storage strategies among bloom-forming diatoms

Robert H. Lampe[a,1], Elizabeth L. Mann[b], Natalie R. Cohen[a,c], Claire P. Till[d], Kimberlee Thamatrakoln[e], Mark A. Brzezinski[f,g], Kenneth W. Bruland[h], Benjamin S. Twining[b], and Adrian Marchetti[a,2]

[a]Department of Marine Sciences, University of North Carolina at Chapel Hill, Chapel Hill, NC 27599; [b]Bigelow Laboratory for Ocean Sciences, East Boothbay, ME 04544; [c]Marine Chemistry and Geochemistry Department, Woods Hole Oceanographic Institution, Woods Hole, MA 02543; [d]Department of Chemistry, Humboldt State University, Arcata, CA 95521; [e]Department of Marine and Coastal Sciences, Rutgers, the State University of New Jersey, New Brunswick, NJ 08901; [f]The Marine Science Institute, University of California, Santa Barbara, CA 93106; [g]Department of Ecology Evolution and Marine Biology, University of California, Santa Barbara, CA 93106; and [h]Department of Ocean Sciences, University of California, Santa Cruz, CA 95064

Edited by Edward A. Boyle, Massachusetts Institute of Technology, Cambridge, MA, and approved November 14, 2018 (received for review April 2, 2018)

Diatoms are prominent eukaryotic phytoplankton despite being limited by the micronutrient iron in vast expanses of the ocean. As iron inputs are often sporadic, diatoms have evolved mechanisms such as the ability to store iron that enable them to bloom when iron is resupplied and then persist when low iron levels are reinstated. Two iron storage mechanisms have been previously described: the protein ferritin and vacuolar storage. To investigate the ecological role of these mechanisms among diatoms, iron addition and removal incubations were conducted using natural phytoplankton communities from varying iron environments. We show that among the predominant diatoms, *Pseudo-nitzschia* were favored by iron removal and displayed unique ferritin expression consistent with a long-term storage function. Meanwhile, *Chaetoceros* and *Thalassiosira* gene expression aligned with vacuolar storage mechanisms. *Pseudo-nitzschia* also showed exceptionally high iron storage under steady-state high and low iron conditions, as well as following iron resupply to iron-limited cells. We propose that bloom-forming diatoms use different iron storage mechanisms and that ferritin utilization may provide an advantage in areas of prolonged iron limitation with pulsed iron inputs. As iron distributions and availability change, this speculated ferritin-linked advantage may result in shifts in diatom community composition that can alter marine ecosystems and biogeochemical cycles.

phytoplankton | iron limitation | *Pseudo-nitzschia* | ferritin | metatranscriptomics

In wide-ranging areas of the ocean, phytoplankton growth is frequently limited by the availability of the micronutrient iron (1, 2). Inputs of iron via atmospheric dust deposition or resuspension of continental shelf sediment during upwelling are spatially and temporally variable, leading to gradients or sporadic episodes of increased iron concentrations (3, 4). From the tropics to the poles, the introduction of iron to iron-limited surface waters is known to stimulate phytoplankton growth usually dominated by large diatoms (5). One cosmopolitan genus of pennate diatoms in particular, *Pseudo-nitzschia*, consistently thrives when iron is added (6). Consequently, certain bloom-forming diatoms have evolved to possess a number of mechanisms that allow them to persist under chronically low iron and rapidly divide when it is reintroduced (7, 8). One such mechanism is the ability to store iron; however, methods for storage are not universal among all diatoms, which in turn may affect iron storage capacities. Two iron storage strategies in diatoms have been previously described: the protein ferritin and vacuoles (8). However, the ecological implications of these different storage mechanisms remain to be investigated in natural communities.

Diatom ferritins are unlike those from other eukaryotes as the gene was acquired via lateral gene transfer from cyanobacteria, some of which use ferritin for long-term storage (9–11). Although ferritin (*FTN*) is present across all four diatom lineages, it appears to be mostly absent from centric diatoms, including many *Thalassiosira* and *Chaetoceros* species, two prominent genera in the ocean (9, 12, 13). Furthermore, evidence suggests that diatom ferritins do not all serve the same functional role. In addition to long-term storage, ferritin may play a role in iron homeostasis. Free intracellular iron is toxic to cells, and some microalgae express ferritin to buffer iron released from degrading proteins (14–16). In the green algae, *Ostreococcus*, ferritin that serves this buffering role was regulated by the circadian clock rather than by iron availability (14). Similarly in some *FTN*-containing diatoms, gene expression changes are comparatively subdued between different iron nutritional states, suggesting a role other than long-term storage (12).

In contrast, *Pseudo-nitzschia* ferritins are highly conserved and, when acclimated to varied iron concentrations, *Pseudo-nitzschia* substantially increase *FTN* expression with dissolved iron concentrations (17, 18). Additionally, the oceanic species *Pseudo-nitzschia granii* was able to perform significantly more cell divisions than the non–ferritin-containing diatom, *Thalassiosira oceanica*, when transitioned from high to low iron conditions (18). As a result, ferritin in *Pseudo-nitzschia* provides an explanation for their unusually high iron storage capacities (12, 18). Biochemical examination of *Pseudo-nitzschia* ferritin, however,

Significance

The availability of the micronutrient iron has profound influences on primary productivity and biogeochemical cycling in the ocean. Here we describe iron storage mechanisms in diatoms, a predominant group of phytoplankton. We substantiate evidence with environmental data that diatoms have evolved to cope with iron limitation by storing iron in different ways. One iron storage mechanism, the protein ferritin, may be well suited for less frequent and pulsed iron inputs. As a result, the diatom community composition may shift to ferritin-using diatoms in potential scenarios where iron availability is reduced.

Author contributions: B.S.T. and A.M. designed research; N.R.C., C.P.T., K.T., M.A.B., K.W.B., B.S.T., and A.M. performed research; R.H.L., E.L.M., B.S.T., and A.M. analyzed data; and R.H.L., E.L.M., B.S.T., and A.M. wrote the paper.

The authors declare no conflict of interest.

This article is a PNAS Direct Submission.

Data deposition: The sequence data reported in this paper have been deposited in the National Center for Biotechnology (NCBI) Sequence Read Archive under accession nos. SRP074302 (BioProject no. PRJNA320398) and SRP108216 (BioProject no. PRJNA388329).

[1]Present address: Integrative Oceanography Division, Scripps Institution of Oceanography, University of California, San Diego, La Jolla, CA 92093.

[2]To whom correspondence should be addressed. Email: amarchetti@unc.edu.

This article contains supporting information online at www.pnas.org/lookup/suppl/doi:10.1073/pnas.1805243115/-/DCSupplemental.

Published online December 11, 2018.

shows that iron remineralization is slow, suggesting a role in buffering (19). Beyond speculation over its true function, the ecological importance of ferritin also remains in question; it has been suggested that competitive strength for diatoms in iron-limited regions lies primarily in using iron-free proteins rather than iron storage (20).

In the non–ferritin-containing species of the genus *Thalassiosira*, evidence supports an intracellular vacuole mechanism for iron storage. *Thalassiosira pseudonana* possesses a divalent transporter belonging to the natural resistance-associated macrophage protein (*NRAMP*) family (21), and some *NRAMP* proteins are used in other eukaryotes to transport iron out of vacuoles (22, 23). Observed up-regulation of this gene under low dissolved iron concentrations suggests that *NRAMP* could be used to mobilize iron out of a vacuole although a role in cell-surface uptake has not been ruled out (21). Anomalously high intracellular regions of iron with stoichiometries consistent with polyphosphate-bound iron in *T. pseudonana* and *Thalassiosira weissflogii* also support a vacuolar storage mechanism for these diatoms (24).

These previous investigations of iron storage were performed in the laboratory where conditions do not fully reflect the natural environment (25). In particular, these laboratory experiments were conducted with monocultures where there is a lack of competition among different diatoms and other phytoplankton groups or interspecies interactions. Advances in analytical capabilities have improved the ability to study the relationship between iron and phytoplankton in natural communities. Reference genomic data for marine organisms allow for annotation of environmental RNA, or metatranscriptomes, including accurate taxonomic annotation for well-represented genera (26). Synchrotron X-ray fluorescence (SXRF) enables quantitative elemental analysis, including that of iron, for individual cells (27). Here we combine metatranscriptomics and SXRF to examine iron storage in specific diatom taxa within natural eukaryotic phytoplankton communities. Using shipboard incubations, iron was added to or removed from phytoplankton with varying initial iron physiological states. We show that iron storage ability can be exceptionally high and that ferritin expression is unique in *Pseudo-nitzschia* while other non–ferritin-using diatoms likely use vacuolar storage. This ferritin-linked storage ability may provide an advantage to ferritin-using diatoms such as *Pseudo-nitzschia* under prolonged periods of iron limitation.

Results and Discussion

Iron States Within the Initial Phytoplankton Communities and Incubations. The iron addition and removal experiments were conducted at four coastal sites and one oceanic site (Fig. 1 and Table 1). Three of the coastal sites are located in the California Upwelling Zone (CUZ): C-High, C-Low1, and C-Low2. In the CUZ, iron delivery is primarily dependent on upwelling-driven resuspension of continental shelf sediments creating a mosaic of iron-limited regions that is largely dependent on shelf width (*SI Appendix*, Fig. S1) (3, 28, 29). The other experiments were conducted along the Line-P transect, a well-characterized iron gradient extending into the high-nutrient low-chlorophyll (HNLC) region of the Northeast Pacific Ocean (30). Specifically, the sites correspond to the coastal station, P4 (P-High), and an oceanic site, Ocean Station Papa or P26 (P-Low).

Herein named based on their initial iron status (high or low), these locations provided varying initial phytoplankton biomass, macronutrient, and iron concentrations that were then further manipulated by the addition of iron (Fe) or the removal of bioavailable iron through addition of the strong iron chelator desferrioxamine B (DFB) (Fig. 2 and Table 1). Short-lived pulse additions were also simulated by an initial addition of iron followed by addition of DFB at the first time point (FeDFB treatments). Iron status was assessed based on oceanographic context (*SI Appendix*), differences in the chemical and biological properties of the seawater [nitrate drawdown, chlorophyll *a*, biogenic silica, and photosynthetic efficiency (F_v:F_m)] (*SI Appendix*, Table S2), and a combination of gene expression-based molecular indicators that evaluate iron stress or limitation for distinct diatom genera (*SI Appendix*, Fig. S2).

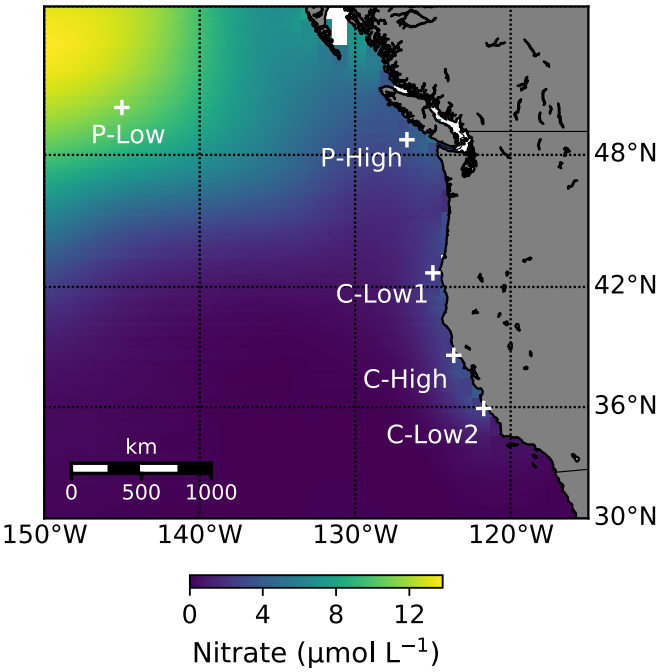

Fig. 1. Map of field incubation locations with interpolated statistical means of nitrate concentrations ($\mu mol \cdot L^{-1}$) on a 1° grid of all decades from World Ocean Atlas 2013 (73).

Low-iron sites displayed comparatively lower Fe:NO_3 ratios (Table 1). Further substantiating their initial status, significant differences between the Fe and control incubations were always observed in photosynthetic efficiency (F_v:F_m) and commonly found for chlorophyll, biogenic silica, nitrate drawdown, and the molecular indicators of iron stress (*SI Appendix*, Table S3). C-High phytoplankton dynamics were largely unaffected by the addition of iron compared with controls as shown by a lack of significant differences, and those at P-High were driven more by macronutrient availability than by iron.

At all sites, significant differences were observed between the Fe and DFB treatments, indicating that low- and high-iron scenarios were created at each site, regardless of the initial iron status. At C-High, nitrate was significantly reduced by iron addition, but the other macronutrients, chlorophyll, and biogenic silica concentrations did not change significantly. However, the molecular indicators validate that the diatom community's physiology was influenced by the addition of DFB, creating a low-iron contrast. The remaining sites show significant differences between the Fe and DFB treatments in nitrate drawdown, chlorophyll, and biogenic silica, although these differences are also not entirely universal, which may be a result of the dissimilar initial conditions. F_v:F_m, however, was consistently reduced by DFB addition as were increases in the molecular indicators, suggesting iron stress in diatoms at all sites in the DFB treatments.

Taxonomic Distributions. Relative taxonomic distributions based on transcript proportions were assessed within the whole community for phylum-based groupings and among diatom genera

Table 1. Incubation site identifiers, location, and initial iron conditions

Name	Latitude and longitude	Fe:NO_3, nmol·L^{-1}:μmol·L^{-1}	Initial Fe, nmol·L^{-1}
C-High	38.7° N, 123.7° W	0.26	3.57
C-Low1	42.7° N, 125.0° W	0.06	1.05
C-Low2	35.9° N, 121.7° W	0.06	1.28
P-High	48.7° N, 126.7° W	0.42	0.64
P-Low	50.0° N, 145.0° W	0.01	0.05

At site P-High, 10 μmol·L^{-1} of NO_3 was added.

(Fig. 3 and *SI Appendix*, Fig. S3). Although transcript proportions may not always relate to cell abundance, they are indicative of the relative activity among groups and within this study are consistent with relative changes in cell abundance based on microscopic counts where performed (31). Diatoms consistently comprised higher relative abundances in the Fe treatments compared with the DFB treatments at the low-iron sites while the opposite was found by the final time points at both high-iron sites (Fig. 3*A*). Although these higher relative transcript proportions at the low-iron sites appear minor (<10%), they may still have translated to a large absolute abundance of certain diatoms. These higher relative abundances were coupled to increases in chlorophyll (>5 μm) and biogenic silica concentrations, indicating that the absolute cellular abundance of diatoms was greater following iron addition rather than simply a shift in proportions (Fig. 2).

This increase in diatom transcript abundance and presumed cellular abundance when iron was added aligns with diatoms' known ability to respond positively when transitioning from low iron to high iron (5). Diatoms were also favored when the environment transitioned from high to low iron as shown by higher relative abundance in the DFB treatments compared with the Fe treatments by the last time points at the high-iron sites (Fig. 3*A*). Regardless of the situation (high iron to low iron or vice versa), diatoms were ultimately able to increase in relative abundance, aligning with their responsiveness to iron availability (32, 33). In the transition from high to low iron, iron storage may play a role in allowing diatoms to continue to divide as growth rates in other taxa slow.

The dominant diatom genera within these experiments were *Chaetoceros*, *Pseudo-nitzschia*, and *Thalassiosira*, which are also among the most common in the open ocean (*SI Appendix*, Fig. S3) (13). When iron was added, *Thalassiosira* generally comprised higher transcript proportions of the diatom community, while inconsistent differences for *Chaetoceros* were observed (Fig. 3*B*). *Chaetoceros* appeared to be favored by iron addition in the coastal low-iron sites while having slightly higher proportions with DFB in the high-iron sites. Interestingly, *Pseudo-nitzschia* consistently had higher transcript proportions in the control and DFB treatments compared with when iron was added. As anticipated from *Pseudo-nitzschia* species' high-iron storage capacities, their ability to store iron may play a role in these shifts. As iron is removed, *Pseudo-nitzschia* can use stored iron to maintain a higher growth rate while other species may not (18).

The exception was the oceanic site, P-Low, where *Pseudo-nitzschia* transcripts greatly increased in the Fe treatment compared with the control and DFB treatments, consistent with previous observations of iron enrichment in HNLC regions (*SI Appendix*, Fig. S3) (6). Here, *Chaetoceros* proportions remained relatively low, but *Thalassiosira* rose in percentage when iron was added as seen at the other sites. Also as observed at the other sites in the DFB treatments, *Pseudo-nitzschia* still increased to become the most prevalent genus, showing that it persisted compared with the other genera although iron was depleted.

Iron Quotas Among Diatom Genera. Cellular iron contents, or quotas, were quantified in individual *Chaetoceros* and *Pseudo-nitzschia* cells from within the incubations using SXRF microscopy (Fig. 4*A* and *SI Appendix*, Fig. S4) (27). Both coastal and oceanic *Pseudo-nitzschia* species are known to have exceptionally high iron storage capacities, (8, 12), which was observed in these experiments (Fig. 4*A*). At C-High, where in situ iron concentrations were highest (Table 1), *Pseudo-nitzschia* had significantly higher quotas in the high-iron treatments (control and Fe) compared with *Chaetoceros* as well as *Pseudo-nitzschia* at the other sites.

In many cases, the quotas in *Pseudo-nitzschia* and *Chaetoceros* were similar. For instance, there were no significant differences in the quotas achieved between the genera at P-High, and both increased their quotas when Fe was added at C-Low1 (Fig. 4*A*). At P-High, although phytoplankton growth was induced by the addition of nitrate (primarily haptophytes), diatoms declined in relative transcript proportions from 24 h to 48 h as silicate concentrations decreased to <1 μmol·L^{-1}, which likely became limiting to diatom growth (Fig. 2 and *SI Appendix*, Fig. S3). With silicate depletion preventing cell division, cells likely accumulated iron in the Fe and control treatments (34) and transitioned toward their minimum quotas in the DFB treatment where dissolved iron was bound to DFB (Fig. 4*A*).

At P-Low, *Pseudo-nitzschia* showed an extraordinary ability to maintain a substantial Fe:C quota of 58 ± 11 μmol:mol in the control treatment even though the initial dissolved iron concentrations were 0.05 nmol·L^{-1} and markers of iron stress were high (*SI Appendix*, Fig. S2). *Pseudo-nitzschia* quotas dropped in response to DFB, confirming that the control community had accessed ambient iron to support quotas above their minimum level. Matching the low transcript abundances for *Chaetoceros* cells at this site, no *Chaetoceros* cells were found in SXRF samples, and therefore corresponding iron quotas could not be measured. Overall, these results align with previous studies showing overlap in iron quotas for diatoms, including *Thalassiosira*, under moderate iron conditions, but *Pseudo-nitzschia* species appear to have higher maximum iron quotas and therefore a greater iron storage capacity (8, 12).

A closer examination of the results at C-Low1 suggests that maintenance of stored iron between the two diatom genera is also not the same. At this site, *Pseudo-nitzschia* appeared to be able to use iron storage to continue to divide and outcompete *Chaetoceros*. As dissolved iron concentrations decreased in the control incubations and indicators of iron stress were exhibited (*SI Appendix*, Fig. S2), *Pseudo-nitzschia* were able to maintain iron quotas (26 ± 7 μmol Fe:mol C) while those in *Chaetoceros* declined (6 ± 2 mol Fe:mol C) from 48 h to 72 h. Meanwhile, chlorophyll, biogenic silica, diatom transcript proportions, and transcript proportions of *Chaetoceros* and *Pseudo-nitzschia* all increased between the same two time points (Fig. 4*B*). Notably, *Pseudo-nitzschia* increased from 26% to 39% of diatom transcripts while *Chaetoceros* remained lower.

In the DFB treatments, *Chaetoceros* quotas at both time points were similar to the control, suggesting that *Chaetoceros* cells reached their minimum quota rapidly as iron was depleted. Although the quotas at 72 h in the DFB treatment were similar in both *Chaetoceros* and *Pseudo-nitzschia*, the reduction in quota for *Pseudo-nitzschia* can be attributed to their proportions approximately doubling over the time frame of the incubations to 40% of diatom transcripts while *Chaetoceros* proportions steadily declined to 4% (Fig. 4*B*). Meanwhile, diatom transcript proportions increased over time from 15% to 21% as did chlorophyll in the large size fraction from 0.70 μg·$L^{-1}$to 1.93 μg·L^{-1}. *Pseudo-nitzschia* were likely able to use their stored iron at 48 h to

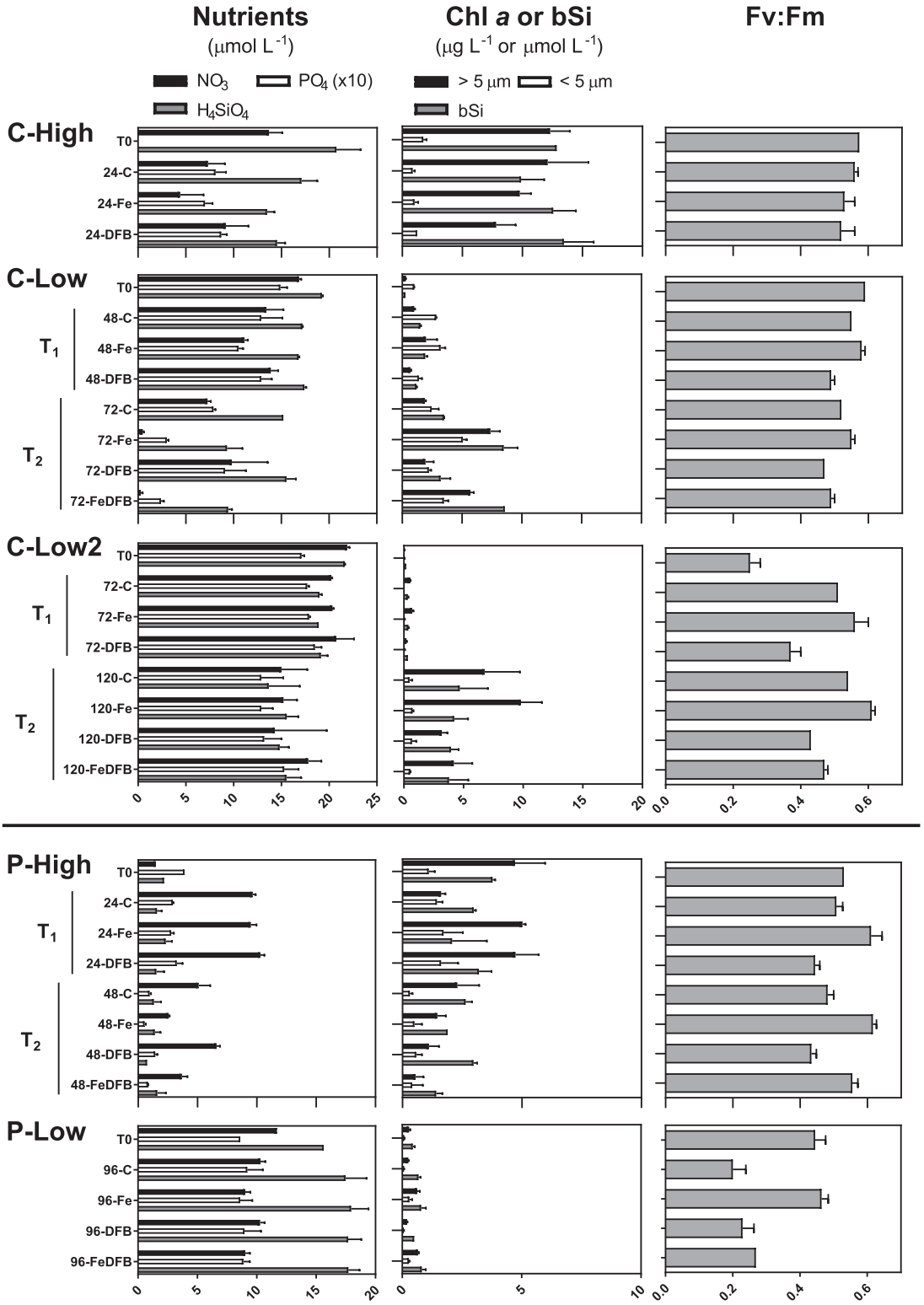

Fig. 2. Macronutrient (μmol·L^{-1}), size-fractionated chlorophyll *a* (μg·L^{-1}), and biogenic silica (μmol·L^{-1}) concentrations and maximum photochemical yields of photosystem II (F_v:F_m) from the initial collected seawater (t = 0) and incubations at various time points. Incubations are labeled as follows: control (C), iron addition (Fe), iron removal (DFB), and iron addition followed by removal (FeDFB) and denoted as the first or second time point (T_1 or T_2) where applicable. CUZ sites and Line-P sites are grouped separately as two of the *x*-axis scales are different.

continue to divide and become a larger proportion matching the control treatment by 72 h despite iron removal by addition of DFB. *Chaetoceros*, on the other hand, lacked stored Fe to draw on at 48 h in the presence of DFB. Taken together, iron storage at this low-iron site likely allowed *Pseudo-nitzschia* to maintain a higher growth rate while *Chaetoceros* growth slowed, consistent with what has been previously observed in laboratory experiments between *P. granii* and *T. oceanica* (18).

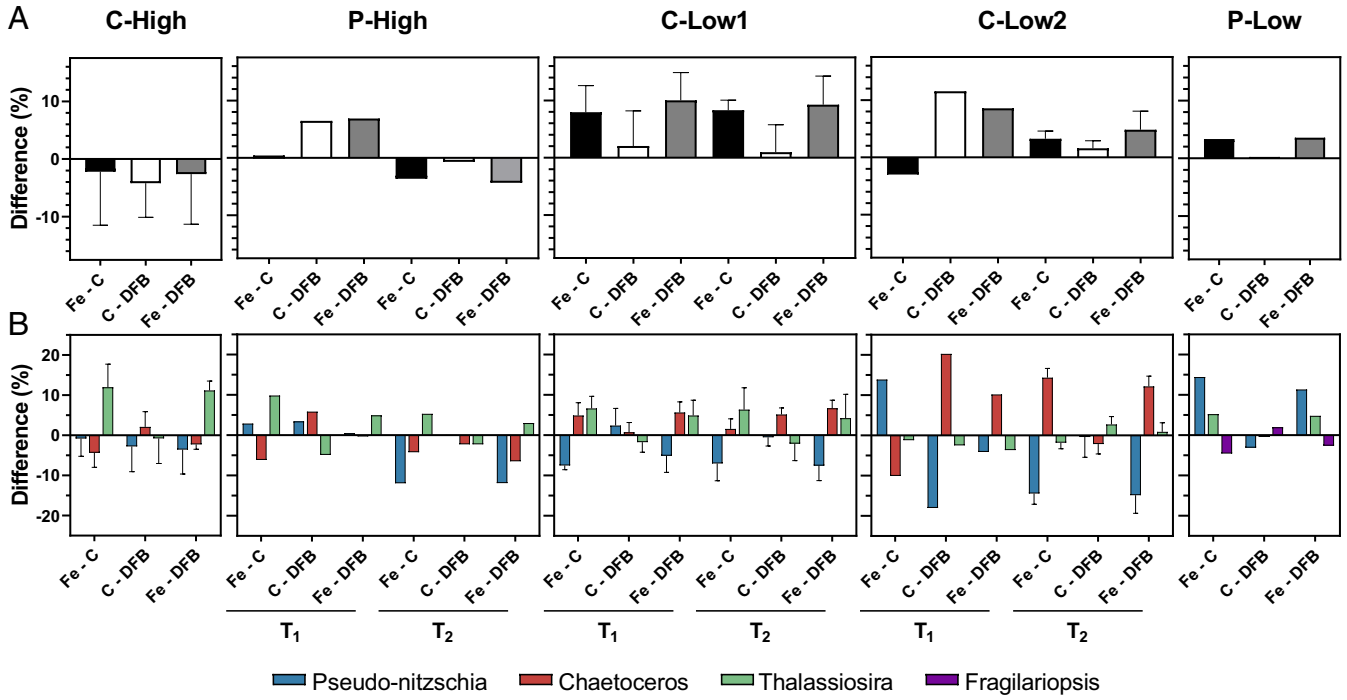

Fig. 3. Differences in relative proportions of taxonomically annotated transcripts between the iron addition and control (Fe-C), control and iron removal (C-DFB), and iron addition and iron removal (Fe-DFB) at each site for (*A*) diatom reads within the total library (Fe-C, black; C-DFB, white; Fe-DFB, gray) and (*B*) *Pseudo-nitzschia* (blue), *Chaetoceros* (red), and *Thalassiosira* (green) within the diatom reads. *Chaetoceros* were a small percentage of the diatom population at P-Low and *Fragilariopsis* (purple) are shown instead. Plots are grouped by initial iron state (high or low).

Ferritin Expression in *Pseudo-nitzschia* and Other Diatoms. Ferritin expression in *Pseudo-nitzschia* was detected at all sites and at comparatively high levels in several incubations, being undetected only in the extreme low-iron scenarios at P-Low and the initial community at C-Low2 that was obtained from below the euphotic zone and thus was severely light limited and contained a low abundance of diatoms (Fig. 5*A* and *SI Appendix*, Fig. S5). Phylogenetic analysis of environmental sequences indicates that these *FTN* sequences belong to both diatom ferritin groups (9) and are derived from multiple *Pseudo-nitzschia* species (*SI Appendix*, Figs. S6 and S7). A previous iron and B-vitamin enrichment experiment at Ocean Station Papa (P-Low) also detected *FTN* expression in *Pseudo-nitzschia* (35); thus, the abundance of *FTN* transcripts across these sites and experiments

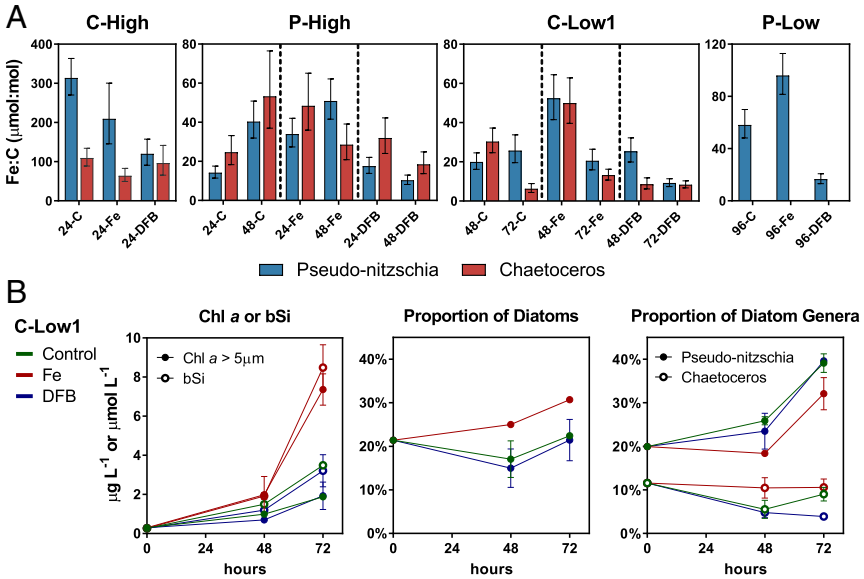

Fig. 4. (*A*) Cellular iron quotas (μmol Fe:mol C) in *Chaetoceros* and *Pseudo-nitzschia* from incubations. Bars are geometric means ± SE. (*B*) Time course for site C-Low1 of chlorophyll *a* (>5 μm size fraction only), biogenic silica, diatom relative transcript proportions, and relative transcript proportions of *Pseudo-nitzschia* and *Chaetoceros* within diatoms. The treatments shown are control (green), iron addition (Fe, red), and iron removal (DFB, blue). Plots are grouped by initial iron state (high or low).

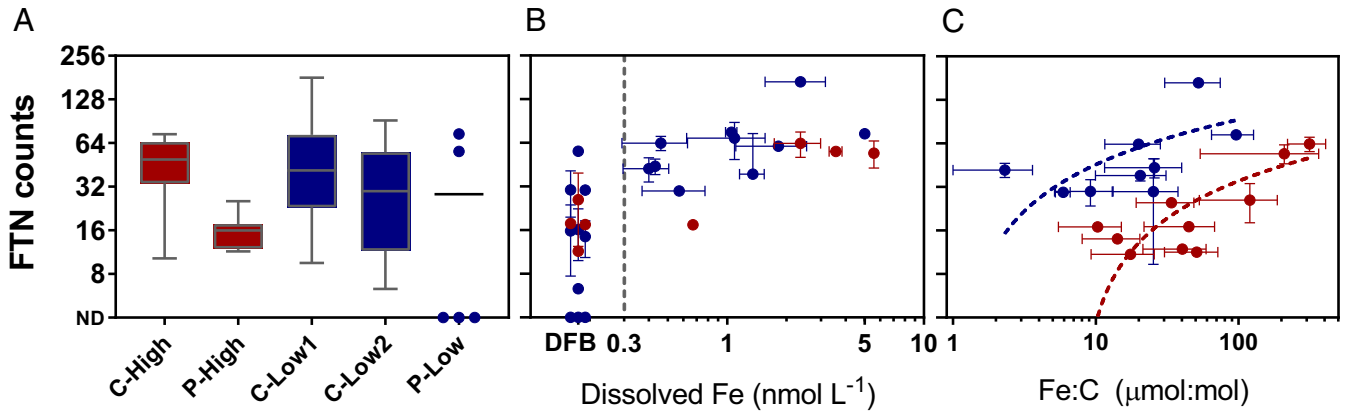

Fig. 5. *Pseudo-nitzschia* normalized ferritin (*FTN*) expression for all initial conditions and incubations. ND, no transcripts detected. Symbols are colored according to high (red)- or low (blue)-iron sites. (*A*) Box plots of *FTN* counts at each site. (*B*) Averaged *FTN* counts as a function of dissolved iron concentrations. In the DFB treatments or where iron was less than 0.05 nmol·L^{-1}, *FTN* counts are plotted to the left of the gray vertical dashed line. (*C*) *FTN* counts as a function of cellular iron content (quota) expressed as Fe:C (μmol:mol) and fitted with a semilog line.

indicates that ferritin utilization is a widespread strategy used by *Pseudo-nitzschia* spp.

Beyond detection, *Pseudo-nitzschia FTN* expression appears to be regulated by their initial iron status. At high-iron sites, comparatively less variation in *FTN* expression was observed even though iron was either added or removed (Fe vs. DFB, Fig. 5*A*). Where replication was available (C-High), these differences were not statistically significant. Conversely, the low-iron sites showed greater variation in *FTN* expression, with the most extreme case being the oceanic site, P-Low. Here, *Pseudo-nitzschia FTN* was undetected in the ambient, severely iron-limited community and then became highly expressed following iron addition (Fig. 5*A*). Certainly, if the primary role of ferritin is for long-term iron storage, it would favor *Pseudo-nitzschia* to minimize synthesis of ferritin unless iron is available in high enough levels to be stored. *Pseudo-nitzschia* strains within environments where iron is low may be adapted to vary their expression of *FTN* to accommodate these ephemeral inputs of iron, whereas *Pseudo-nitzschia* in high-iron environments appear to constitutively express *FTN* to accommodate the more frequent iron inputs and higher supply.

In general, *FTN* expression in *Pseudo-nitzschia* declined under low-iron concentrations and reached a maximal level of expression at dissolved Fe concentrations over 1 nmol·L^{-1} (Fig. 5*B*). This expression pattern matches previous laboratory experiments that used iron chelators to control iron availability (17, 18) and is unlike expression in *Ostreococcus* where ferritin serves a role in recycling intracellular iron (14). Although not tested to higher concentrations here, these data support the hypothesis that *Pseudo-nitzschia* use *FTN* for long-term storage, as *FTN* is likely expressed to maintain storage needed for their maximum quotas. Further substantiating this role, there is a significant positive correlation (Pearson) between *FTN* expression and iron quotas (Fig. 5*C*) as well as the changes in *FTN* expression and iron quotas (*SI Appendix*, Fig. S8). This concordance in *Pseudo-nitzschia FTN* expression and iron quotas supports increased storage of iron as ferritin abundance increases.

Comparisons between the Fe and DFB treatments at each site display these changes in expression in greater detail (Fig. 6). *FTN* expression was always higher when iron was added and lower when it was removed except at the second time point of P-High, which was likely influenced by macronutrient depletion (12). *FTN* was highly expressed in the low-iron sites following iron addition, consistent with *Pseudo-nitzschia* increasing *FTN* expression in response to increased iron concentrations (17, 18). Responses varied when comparing the first and second time points in the Fe treatments, from a significant decrease in transcript abundance at C-Low1 to little change at C-Low2 (Fig. 6). The strong difference at C-Low1 is largely driven by unusually high *FTN* expression at the first time point, being much higher than any other level of *FTN* expression even at high dissolved iron concentrations (Fig. 5*B*). This result may be an artifact of earlier timing of sampling. As noted in a previous laboratory study, maximal expression of *FTN* quickly followed iron resupply to iron-limited *Pseudo-nitzschia multiseries* and then gradually returned to steady-state levels (18). This difference over time could also be affected by macronutrient depletion at the second time point (Fig. 2) (12).

As expected, *FTN* expression was similar between the first and second time points where only DFB was added as the low-iron status of *Pseudo-nitzschia* in the incubations remained constant. In the cases where DFB was added after Fe (FeDFB), *FTN* expression decreased following the addition of DFB at the low-iron sites and matched expression within the DFB-only treatments. The exception was at P-Low where expression of *FTN* remained high and only marginally lower than that in the Fe treatment although DFB had been added for 48 h, suggesting that these oceanic diatoms display a delayed response to iron removal. Once more, these gene expression patterns are consistent with what has been observed for *Pseudo-nitzschia* in the laboratory (17, 18), substantiating that members of this genus use ferritin for long-term storage of iron.

To examine the prevalence of ferritin utilization in other dominant diatoms, *FTN* expression was examined in *Chaetoceros* and *Thalassiosira* (Fig. 6). *FTN* was virtually undetected in *Chaetoceros* with only two assigned contigs from the assembly with low read counts. Phylogenetic analysis shows that these contigs are similar to the reference *FTN* sequence from *Chaetoceros dichaeta* (*SI Appendix*, Fig. S9). As *FTN* sequences have been identified in only a few reference *Chaetoceros* transcriptomes, this result was anticipated (12). Only a few *Thalassiosira* species have been found to possess *FTN*, and *Thalassiosira FTN* was detected only in low abundances (*SI Appendix*, Figs. S5 and S10) with no significant changes in expression (Fig. 6). Previous studies have also observed minute changes in *Thalassiosira FTN* expression as a function of iron status apart from one *FTN* homolog in *Thalassiosira rotula* that had higher expression under iron-limited conditions, suggesting a role other than long-term iron storage in this diatom (12). Among these predominant diatom genera, *Pseudo-nitzschia* appears to be the distinct utilizer of *FTN* for long-term iron storage in its natural environment, whereas the other diatoms are potentially using other mechanisms to store iron.

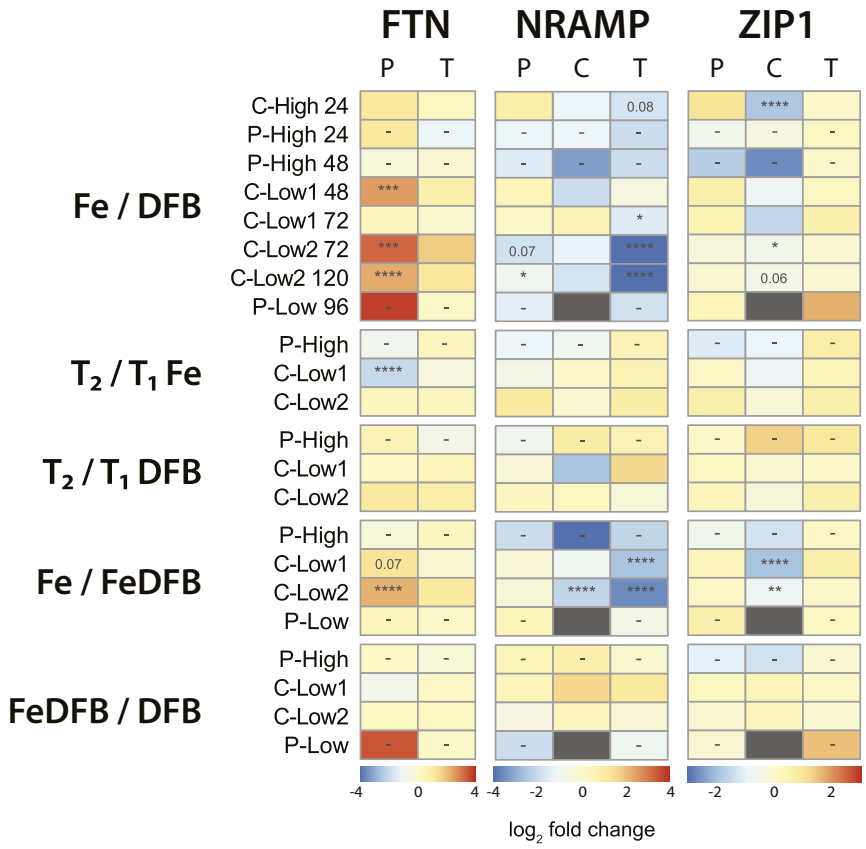

Fig. 6. Heatmap of $\log_2$ fold-change values for ferritin (*FTN*), natural resistance-associated macrophage protein (*NRAMP*), and *ZIP1* expression in *Pseudo-nitzschia* (P), *Chaetoceros* (C), and *Thalassiosira* (T). Comparisons are separated into five groups in order from *Top* to *Bottom*: iron addition (Fe) vs. iron removal (DFB), T_2 Fe vs. T_1 Fe, T_2 DFB vs. T_1 DFB, iron addition and then removal (FeDFB) vs. Fe, and FeDFB vs. DFB. Dark gray indicates that the gene was not detected in both samples being compared. Significance in differential expression is shown within each cell where applicable (displayed numerically, $P \leq 0.1$; $*P \leq 0.05$; $**P \leq 0.01$; $***P \leq 0.001$; $****P \leq 0.0001$; —, not applicable).

Vacuolar-Associated Gene Expression. Expression of *NRAMP* was investigated as it may be related to vacuolar storage of iron. This relationship is based on evidence that some *NRAMP* orthologs in other eukaryotes may be involved in vacuolar storage (22, 23). *Thalassiosira NRAMP* has also been found to be up-regulated when iron quotas and iron concentrations are low (21). As *NRAMP* is a nonspecific divalent metal transporter and Fe uptake in *Thalassiosira* was not inhibited by other divalent metals, *NRAMP* may not be a surface transporter and rather one for transporting iron out of vacuoles (21). The presence of iron contained within vacuoles is also supported by spatial elemental analysis of certain non–ferritin-containing *Thalassiosira* species (24).

Thalassiosira was the genus with the highest and most significant differential expression of *NRAMP* (Fig. 6 and *SI Appendix*, Fig. S5). Expression in the other two genera was typically low, not significantly different, and inconsistent between treatments, indicating that the use of *NRAMP* may be distinct to *Thalassiosira* among the three examined diatom genera, much like *FTN* in *Pseudo-nitzschia*. Interestingly, *Pseudo-nitzschia* showed higher expression only at P-Low, albeit with low differential expression between treatments (*SI Appendix*, Fig. S5). It is possible that these subarctic oceanic *Pseudo-nitzschia* spp. constitutively express *NRAMP* as a low-affinity metal permease on the cell surface. For these diatoms, this function would be advantageous at this site as iron availability is extremely growth limiting, Fe(II) oxidation rates are slower in colder waters, and Fe(II) may account for a significant amount of the total dissolved iron (36). High expression of *NRAMP* in the low-iron treatments at this site was also observed in the closely related genus *Fragilariopsis*, indicating that it may serve a similar role (*SI Appendix*, Fig. S11).

Thalassiosira consistently demonstrated higher *NRAMP* transcript abundance in the DFB treatments with some significant differential expression (Fig. 6). Expression was consistent when comparing across time in the Fe or DFB treatments. In the iron addition and then removal treatment (FeDFB), expression was significantly higher compared with that in the Fe treatment. Low differences in expression were observed between the FeDFB treatment and the DFB treatment. These results are consistent with the laboratory studies showing higher *NRAMP* expression under low-iron concentrations and significant down-regulation following iron resupply in *T. pseudonana* (21); thus, they are consistent with what we may expect from the role of *NRAMP* in transporting iron out of a vacuole. In particular, the high expression in the FeDFB treatment suggests that *Thalassiosira* store iron in vacuoles and then highly express this transporter to shuttle iron out of the vacuole once it is no longer externally available. Given the rapid responsiveness to iron availability observed in the laboratory (21) and the differential expression observed here, it appears likely that *NRAMP* expression is regulated by external iron availability rather than cellular iron quota.

Although this expression supports common use of this vacuolar strategy in *Thalassiosira*, the role of *NRAMP* in diatoms remains rather elusive and may be different between genera as is evident from its expression in ferritin-using, oceanic *Pseudo-nitzschia* (Fig. 6). Phylogenetic analysis of diatom *NRAMP* genes shows that they appear conserved to some degree among diatoms, distinct from *NRAMPs* in other organisms, and to have

originated from their red algal ancestor (*SI Appendix*, Fig. S12). The gene, however, is not universal to all diatoms given that an ortholog was not detected in the *Phaeodactylum tricornutum* genome (37).

Overall, *Chaetoceros* displayed little *FTN* or *NRAMP* expression in these incubations, but iron quotas were similar to that of *Pseudo-nitzschia* within most treatments, particularly at C-Low1 and P-High (Figs. 4 and 6 and *SI Appendix*, Fig. S5). From these quotas, it is apparent that *Chaetoceros* is able to store iron at quantities similar to that of *Pseudo-nitzschia* within these time frames; however, their iron storage mechanism remains unknown. High expression of *NRAMP* in *Chaetoceros* was found in the FeDFB treatments at C-Low2, but not at C-Low1. The difference appears to be pronounced at P-High, but this result is an artifact of no detection in the Fe treatment (Fig. 6 and *SI Appendix*, Fig. S5). It is possible that there was some *NRAMP* utilization by *Chaetoceros* at certain sites, but this response was not consistently found.

Expression of other iron-related genes that show similar patterns to *FTN* and *NRAMP* were queried. In addition to *NRAMP*, diatoms possess divalent metal transporters belonging to the ZIP family (38). Like *NRAMP*, these may also be localized to the cell or vacuolar membrane for passive metal transport, including that of Fe(II) (39). Expression of two *ZIP* orthologs (*ZIP1* and *ZIP7*) was detected in all three dominant genera in the metatranscriptomes. *ZIP7* was expressed most by *Pseudo-nitzschia* but not differentially expressed among treatments (*SI Appendix*, Fig. S13). Unlike *FTN* and *NRAMP*, *ZIP1* was expressed at similar levels on average among the three genera; however, *Chaetoceros* was the only predominant diatom to significantly modify expression of the gene in relation to its iron status (Fig. 6). Furthermore, this expression pattern is similar to that of *NRAMP* where increased transcript abundance is observed when DFB is added, particularly when transitioning from high to low iron as in the high-iron sites and the FeDFB treatments. As a result, we speculate that *Chaetoceros* may also use a vacuolar storage mechanism but potentially uses a different transporter protein, ZIP1, for transport out of the vacuole. This gene appears to be similar to one present in some other heterokonts and green algae, suggesting different evolutionary origins from *NRAMP* or *FTN* (*SI Appendix*, Fig. S14).

Furthermore, the mechanism of iron import into the vacuole is unknown. Diatoms possess a homolog of the vacuolar iron transporter, *VIT1* or *CCC1*, used for this purpose in *Arabidopsis thaliana* and *Saccharomyces cerevisiae*, respectively (40, 41). Expression of these genes was found to be low and inconsistent among treatments in our incubations. Previous experiments show that one of the homologs in *P. tricornutum* was significantly regulated by cadmium; therefore, it is possible that *VIT1* is not related to iron transport in diatoms (40).

Biogeochemical and Ecological Implications. The expression of *FTN* in *Pseudo-nitzschia* and *NRAMP* in *Thalassiosira* in these natural communities is consistent with previous laboratory studies substantiating these distinct iron storage strategies—ferritin and vacuolar storage—in ecologically important diatom genera. Of the three main diatom genera in this study, *Pseudo-nitzschia* was the unique utilizer of *FTN*, explaining *Pseudo-nitzschia*'s high iron storage capacity (12, 18). Meanwhile, *NRAMP* was the most highly expressed and regulated in *Thalassiosira*. Transcripts for neither of these genes were abundant in *Chaetoceros* although iron quotas in *Chaetoceros* were often similar to those in *Pseudo-nitzschia*, leading to speculation that *Chaetoceros* uses a different divalent metal transporter, *ZIP1*, for vacuolar iron storage. Interestingly, the presence of these three genes in diatoms also appears to have different evolutionary origins: lateral gene transfer (*FTN*), the red algal ancestor (*NRAMP*), or the green algal ancestor (*ZIP1*). Since ferritin likely originated from a lateral gene transfer event from cyanobacteria, but it is present in all four diatom classes (9, 18), we hypothesize that it was inherited by a diatom ancestor before the first divergence of these lineages ∼56 Mya (7). Contributing to diatom diversification, many centric diatoms may have maintained a vacuolar storage mechanism whereas ancestral diatoms to *Pseudo-nitzschia* and *Fragilariopsis* switched to using ferritin for long-term storage and have conserved the gene. As other diatoms maintained a vacuolar storage mechanism, ferritin genes may be absent as a result of gene loss events or present for functions other than long-term iron storage (12).

Ferritin in the closely related pennate diatom *Fragilariopsis* is believed to serve the same function as ferritin in *Pseudo-nitzschia* (18). In laboratory studies with *Fragilariopsis cylindrus* and *Fragilariopsis kerguelensis*, ferritin expression was higher under steady-state iron-replete conditions compared with iron-limited conditions (17, 42). *Fragilariopsis* ferritin expression in the field experiments described here was relatively low and inconsistent, but *Fragilariopsis* were not abundant within the incubations (*SI Appendix*, Fig. S11). Other metatranscriptomes also show conflicting results ranging from absent in one study from the Southern Ocean (42), to very low abundances in another study at P-Low (35), to abundant but not differentially expressed in another Southern Ocean metatranscriptome (43). Considering the relatively slow growth rate of *Fragilariopsis* from polar environments (17), timing of sampling may underlie the lack of observed transcriptomic responses in the field compared with steady-state laboratory conditions. Examining *Fragilariopsis* transcriptional changes of iron-responsive genes such as *FTN* over time following iron supply would provide context for these results.

The advantage of iron storage via ferritin vs. vacuolar storage is likely most beneficial in regions of ephemeral iron supply where iron can be accumulated following a pulsed input and then passed on to progeny. As observed from artificial iron enrichments, new inputs can be short-lived with a majority of the iron being lost to dispersion or sinking with inorganic particles (44, 45). Dissolved iron as well as the relative contributions of external and recycled Fe (i.e., the *fe* ratio) (46) can change in a period of just a few days (47). As a result, diatoms likely must compete for and quickly assimilate a relatively small proportion of total new dissolved iron (48). While recycled iron may sustain prolonged growth (44), iron uptake in later bloom stages can be dominated by other phytoplankton groups, suggesting that other small microbes may outcompete diatoms for regenerated iron (25) and highlighting the ecological importance of accessing and storing initial inputs of new iron for diatoms.

Iron within ferritin can be stored rapidly and effectively in relatively high quantities, which enables ferritin-using diatoms to sustain continued growth for longer periods of time across large spatial distances while avoiding cellular iron toxicity (49). Ferritin may also enable more uniform distribution of stored iron to daughter cells compared with a vacuole as the protein with stored iron may be more readily transferred to daughter cells during cell division. Indeed, the apparent ferritin-using diatoms *Pseudo-nitzschia* and *Fragilariopsis* have dominated iron-enrichment experiments in the subarctic Pacific and Southern Oceans (6, 33). Low-iron sites and treatments here also tended to favor *Pseudo-nitzschia* (Fig. 3). *Fragilariopsis* is also known to be abundant in the Southern Ocean, particularly in the open ocean regions where iron delivery is more sporadic and pulsed (50, 51). These genera can maintain higher growth rates, enabling a larger initial bloom as well as a larger and longer-lasting seed population until the next iron deposition event occurs.

Iron distributions and availability will likely be altered as a result of climate change (52). In some areas increases in surface iron are predicted as a result of increased combustion emissions of metals, dust from land use and climate changes,

enhanced vertical supply of iron, or trapping of iron near the surface from increased stratification (4, 53, 54). Lower biological production may result in increases in dissolved iron as well (55). However, elevated iron deposition may be offset by other factors. Coastal upwelling environments such as the California-based sites in this study may see more widespread iron limitation (56). Potential increases in upwelled nitrate inputs could be unmatched by new iron inputs which will further exaggerate existing iron-limited regions or drive others into an iron-limited state (57). Ocean acidification will likely result in less bioavailable iron for diatoms as the release of dissolved iron from certain organic ligands is reduced under lower pH (58), and high-affinity iron uptake via phytotransferrin in diatoms is significantly impacted by decreased carbonate concentrations (59). Moreover, uncertainty remains in regard to how acidification will affect other factors governing iron solubility and availability such as the production of siderophores by heterotrophic bacteria (60).

If prolonged iron limitation occurs with greater frequency, there will be a shift toward a system like that observed at P-Low where increases in ferritin-using diatoms such as *Pseudo-nitzschia* in these areas or potentially *Fragilariopsis* in the Southern Ocean are anticipated from gaining longer-lasting seed populations due to enhanced iron storage. *Pseudo-nitzschia* in coastal regions are also known for their synthesis of the neurotoxin domoic acid (DA), potentially favoring a system more conducive to its production and leading to an increase in frequency and intensity of harmful algal blooms (61). DA was detected in all CUZ incubations with concentrations up to 3.00 ng·mL^{-1} (*SI Appendix*, Fig. S15) (32). Furthermore, *Fragilariopsis* can contribute to high biogenic opal burial in the Southern Ocean, suggesting an enhancement in the silica pump (50, 62). Beyond simply the impact that iron limitation has on primary productivity, these long-term community shifts toward ferritin-using diatoms would further influence the marine food web structure and associated biogeochemical cycles.

Materials and Methods

Incubation experiments were conducted at five sites within the CUZ (July 2014) or along the Line-P transect in the subarctic Northeast Pacific Ocean (June 2015) (Fig. 1 and Table 1). Near-surface water (*SI Appendix*, Table S1) was collected using trace-metal clean techniques and distributed into acid-cleaned 10-L Cubitainers except in C-Low2 for which water was collected from 96 m. Cubitainers were incubated on deck at near-ambient surface water temperature and screened at approximately one-third surface irradiance. Treatments included an unamended control (C), addition of iron with 5 nmol·L^{-1} $FeCl_3$ (Fe), removal of iron with 200 nmol·L^{-1} of the siderophore DFB, and iron addition at t = 0 followed by iron removal at the first time point (FeDFB) to mimic a short-lived iron pulse. At site P-Low, DFB was added to a control and Fe treatment at 48 h for the DFB and FeDFB treatment sampled at 96 h. At site P-High, 10 μmol·L^{-1} of NO_3 was added to all incubations to support growth since initial NO_3 concentrations were low. At dawn of each time point, triplicate Cubitainers of each treatment were harvested and subsamples were collected for the following measurements: dissolved inorganic nutrients, chlorophyll *a*, biogenic silica, F_v:F_m, RNA, and SXRF.

RNA was extracted using the ToTALLY RNA Total RNA Isolation Kit, and mRNA was sequenced on an Illumina HiSeq 2000. All samples were sequenced in triplicate except samples for treatments with low yields (all t = 0 and Line-P samples), where triplicate extractions were pooled into one sample. Reads were assembled into contigs with ABySS v1.5.2 (63) and were annotated de novo using BLASTX v2.2.31. For functional annotation, Kyoto Encyclopedia of Genes and Genomes (KEGG) (64) assignments were used whereas taxonomic classification was assigned using MarineRefII, a custom reference database that includes the transcriptomes from the Marine Microbial Eukaroyte Transcriptome Sequence Project (65). Read counts were estimated using Salmon v0.73 (66). Normalization, gene expression, and differential expression were then assessed within each genera using DESeq2 v.1.12.4 (67).

SXRF samples were collected and analyzed following Twining et al. (27, 68). Briefly, cells from 500 mL of sample were preserved with 0.25% trace-metal clean electron-microscopy grade buffered glutaraldehyde and centrifuged onto C/formvar-coated Au transmission electron microscopy (TEM) grids. Light and chlorophyll fluorescence images were collected for target cells, using a shipboard microscope. SXRF analyses were performed at the 2-ID-E microprobe beamline at the Advanced Photon Source (Argonne National Laboratory). The incident beam energy was tuned to 10 keV to allow for the stimulation of K-line emissions for all elements ranging in atomic number from Si through Zn. Element concentrations were calculated by comparison with certified reference standards (27, 69), and cellular C was calculated from cell volume (70).

Methods for analyzing chlorophyll *a*, biogenic silica, and F_v:F_m are described in Cohen et al. (35). Sequence data have been deposited in the NCBI Sequence Read Archive under accession numbers SRP074302 and SRP108216 (71, 72). Additional materials and methods are provided in *SI Appendix*.

ACKNOWLEDGMENTS. We thank the captain and crew of the *R/V Melville* and the *CCGS J. P. Tully* as well as the participants of the IRNBRU (MV1405) cruise for the California-based data, particularly K. Ellis [University of North Carolina (UNC)], T. Coale (University of California, San Diego), F. Kuzminov (Rutgers), H. McNair [University of California, Santa Barbara (UCSB)], and J. Jones (UCSB). W. Burns (UNC), S. Haines (UNC), and S. Bargu (Louisiana State University) assisted with sample processing and analysis. This work was funded by the National Science Foundation Grants OCE-1334935 (to A.M.), OCE-1334632 (to B.S.T.), OCE-1333929 (to K.T.), OCE-1334387 (to M.A.B.), OCE-1259776 (to K.W.B), and DGE-1650116 (Graduate Research Fellowship to R.H.L).

1. Martin JH, Fitzwater SE (1988) Iron deficiency limits phytoplankton growth in the north-east Pacific subarctic. *Nature* 331:341–343.
2. Moore JK, Doney SC, Glover DM, Fung IY (2001) Iron cycling and nutrient-limitation patterns in surface waters of the world ocean. *Deep Sea Res Pt II* 49:463–507.
3. Bruland KW, Rue EL, Smith GJ (2001) Iron and macronutrients in California coastal upwelling regimes: Implications for diatom blooms. *Limnol Oceanogr* 46:1661–1674.
4. Mahowald NM, et al. (2018) Aerosol trace metal leaching and impacts on marine microorganisms. *Nat Commun* 9:2614.
5. Boyd PW, et al. (2007) Mesoscale iron enrichment experiments 1993-2005: Synthesis and future directions. *Science* 315:612–617.
6. de Baar HJW, et al. (2005) Synthesis of iron fertilization experiments: From the iron age in the age of enlightenment. *J Geophys Res Oceans* 110:C09S16.
7. Armbrust EV (2009) The life of diatoms in the world's oceans. *Nature* 459:185–192.
8. Marchetti A, Maldonado MT (2016) *Iron*, eds Borowitzka MA, Beardall J, Raven JA (Springer International Publishing, Cham, Switzerland), pp 233–279.
9. Groussman RD, Parker MS, Armbrust EV (2015) Diversity and evolutionary history of iron metabolism genes in diatoms. *PLoS One* 10:e0129081.
10. Keren N, Aurora R, Pakrasi HB (2004) Critical roles of bacterioferritins in iron storage and proliferation of cyanobacteria. *Plant Physiol* 135:1666–1673.
11. Shire DM, Kustka AB (2015) Luxury uptake, iron storage and ferritin abundance in *Prochloroccocus marinus* (Synechococcales) strain MED4. *Phycologia* 54:398–406.
12. Cohen NR, et al. (2018) Iron storage capacities and associated ferritin gene expression among marine diatoms. *Limnol Oceanogr* 63:1677–1691.
13. Malviya S, et al. (2016) Insights into global diatom distribution and diversity in the world's ocean. *Proc Natl Acad Sci USA* 113:E1516–E1525.
14. Botebol H, et al. (2015) Central role for ferritin in the day/night regulation of iron homeostasis in marine phytoplankton. *Proc Natl Acad Sci USA* 112:14652–14657.
15. Liochev SI, Fridovich I (1999) Superoxide and iron: Partners in crime. *IUBMB Life* 48:157–161.
16. Long JC, Sommer F, Allen MD, Lu SF, Merchant SS (2008) FER1 and FER2 encoding two ferritin complexes in *Chlamydomonas reinhardtii* chloroplasts are regulated by iron. *Genetics* 179:137–147.
17. Marchetti A, et al. (2017) Development of a molecular-based index for assessing iron status in bloom-forming pennate diatoms. *J Phycol* 53:820–832.
18. Marchetti A, et al. (2009) Ferritin is used for iron storage in bloom-forming marine pennate diatoms. *Nature* 457:467–470.
19. Pfaffen S, et al. (2015) A diatom ferritin optimized for iron oxidation but not iron storage. *J Biol Chem* 290:28416–28427.
20. Mock T, Medlin LK (2012) Genomics and genetics of diatoms. *Adv Bot Res* 64:245–284.
21. Kustka AB, Allen AE, Morel FMM (2007) Sequence analysis and transcriptional regulation of iron acquisition gens in two marine diatoms. *J Phycol* 43:715–729.
22. Lanquar V, et al. (2005) Mobilization of vacuolar iron by AtNRAMP3 and AtNRAMP4 is essential for seed germination on low iron. *EMBO J* 24:4041–4051.
23. Portnoy ME, Liu XF, Culotta VC (2000) *Saccharomyces cerevisiae* expresses three functionally distinct homologues of the nramp family of metal transporters. *Mol Cell Biol* 20:7893–7902.
24. Nuester J, Vogt S, Twining BS (2012) Localization of iron within centric diatoms of the genus *Thalassiosira*. *J Phycol* 48:626–634.
25. Boyd PW, et al. (2015) Why are biotic iron pools uniform across high- and low-iron pelagic ecosystems? *Glob Biogeochem Cy* 29:1028–1043.

26. Caron DA, et al. (2017) Probing the evolution, ecology and physiology of marine protists using transcriptomics. *Nat Rev Microbiol* 15:6–20.
27. Twining BS, et al. (2003) Quantifying trace elements in individual aquatic protist cells with a synchrotron x-ray fluorescence microprobe. *Anal Chem* 75:3806–3816.
28. Hutchins DA, DiTullio GR, Zhang Y, Bruland KW (1998) An iron limitation mosaic in the California upwelling regime. *Limnol Oceanogr* 43:1037–1054.
29. Till CP, et al. (August 27, 2018) The iron limitation mosaic in the California current system: Factors governing Fe availability in the shelf/near-shelf region. *Limnol Oceanogr*, doi.org/10.1002/lno.11022.
30. Harrison PJ (2002) Station Papa time series: Insights into ecosystem dynamics. *J Oceanography* 58:259–264.
31. Lampe RH, et al. (2018) Divergent gene expression among phytoplankton taxa in response to upwelling. *Environ Microbiol* 20:3069–3082.
32. Cohen NR, et al. (2017) Variations in diatom transcriptional responses to changes in iron availability across ocean provinces. *Front Mar Sci* 4:360.
33. Marchetti A, et al. (2012) Comparative metatranscriptomics identifies molecular bases for the physiological responses of phytoplankton to varying iron availability. *Proc Natl Acad Sci USA* 109:E317–E325.
34. Droop MR (1973) Some thoughts on nutrient limitation in algae. *J Phycol* 9:264–272.
35. Cohen NR, et al. (2017) Iron and vitamin interactions in marine diatom isolates and natural assemblages of the Northeast Pacific Ocean. *Limnol Oceanogr* 62:2076–2096.
36. Roy EG, Wells ML, King DW (2008) Persistence of iron(II) in surface waters of the western subarctic Pacific. *Limnol Oceanogr* 53:89–98.
37. Rastogi A, et al. (2018) Integrative analysis of large scale transcriptome data draws a comprehensive landscape of *Phaeodactylum tricornutum* genome and evolutionary origin of diatoms. *Sci Rep* 8:4834.
38. Allen AE, et al. (2008) Whole-cell response of the pennate diatom *Phaeodactylum tricornutum* to iron starvation. *Proc Natl Acad Sci USA* 105:10438–10443.
39. Eide DJ (2005) *The Zip Family of Zinc Transporters*, eds Iuchi S, Kuldell N (Springer US, Boston), pp 261–264.
40. Brembu T, Jorstad M, Winge P, Valle KC, Bones AM (2011) Genome-wide profiling of responses to cadmium in the diatom *Phaeodcatylum tricornutum*. *Environ Sci Technol* 45:7640–7647.
41. Kim SA, et al. (2006) Localization of iron in *Arabidopsis* seed requires the vacuolar membrane transporter VIT1. *Science* 314:1295–1298.
42. Mock T, et al. (2017) Evolutionary genomics of the cold-adapted diatom *Fragilariopsis cylindrus*. *Nature* 541:536–540.
43. Bertrand EM, et al. (2015) Phytoplankton–bacterial interactions mediate micronutrient colimitation at the coastal Antarctic sea ice edge. *Proc Natl Acad Sci USA* 112:9938–9943.
44. Bowie AR, et al. (2001) The fate of added iron during a mesoscale fertilisation experiment in the Southern Ocean. *Deep Sea Res Pt II* 48:2703–2743.
45. Wong CS, et al. (2006) Iron speciation and dynamics during series, a mesoscale iron enrichment experiment in the NE pacific. *Deep Sea Res Pt II* 53:2075–2094.
46. Boyd PW, et al. (2005) FeCycle: Attempting an iron biogeochemical budget from a mesoscale SF_6 tracer experiment in unperturbed low iron waters. *Glob Biogeochem Cy* 19:GB4S20.
47. Boyd PW, Ellwood MJ, Tagliabue A, Twining BS (2017) Biotic and abiotic retention, recycling and remineralization of metals in the ocean. *Nat Geosci* 10:167–173.
48. Boyd PW, et al. (2012) Microbial control of diatom bloom dynamics in the open ocean. *Geophys Res Lett* 39:L18601.
49. Boyd PW, Mackie D (2008) Comment on "the Southern Ocean biological response to aeolian iron deposition". *Science* 319:159.
50. Abelmann A, Gersonde R, Cortese G, Kuhn G, Smetacek V (2006) Extensive phytoplankton blooms in the Atlantic sector of the glacial Southern Ocean. *Paleoceanography* 21:PA1013.
51. Armand LK, Cornet-Barthaux V, Mosseri J, Queguiner B (2008) Late summer diatom biomass and community structure on and around the naturally iron-fertilised Kerguelen plateau in the Southern Ocean. *Deep Sea Res Pt II* 55:653–676.
52. Hutchins DA, Boyd PW (2016) Marine phytoplankton and the changing ocean iron cycle. *Nat Clim Change* 6:1072–1079.
53. Leung S, Cabré A, Marinov I (2015) A latitudinally banded phytoplankton response to 21st century climate change in the Southern Ocean across the CMIP5 model suite. *Biogeosciences* 12:5715–5734.
54. Moore JK, et al. (2018) Sustained climate warming drives declining marine biological productivity. *Science* 359:1139–1143.
55. Boyd PW, Lennartz ST, Glover DM, Doney SC (2014) Biological ramifications of climate-change-mediated oceanic multi-stressors. *Nat Clim Change* 5:71–79.
56. Capone DG, Hutchins DA (2013) Microbial biogeochemistry of coastal upwelling regimes in a changing ocean. *Nat Geosci* 6:711–717.
57. Rykaczewski RR, Dunne JP (2010) Enhanced nutrient supply to the California current ecosystem with global warming and increased stratification in an earth system model. *Geophys Res Lett* 37:L21606.
58. Shi D, Xu Y, Hopkinson BM, Morel FMM (2010) Effect of ocean acidification on iron availability to marine phytoplankton. *Science* 327:676–679.
59. McQuaid JB, et al. (2018) Carbonate-sensitive phytotransferrin controls high-affinity iron uptake in diatoms. *Nature* 555:534–537.
60. Hoffmann LJ, Breitbarth E, Boyd PW, Hunter KA (2012) Influence of ocean warming and acidification on trace metal biogeochemistry. *Mar Ecol Prog Ser* 470:191–205.
61. Lelong A, Hégaret H, Soudant P, Bates SS (2012) *Pseudo-nitzschia* (Bacillariophyceae) species, domoic acid and amnesic shellfish poisoning: Revisiting previous paradigms. *Phycologia* 51:168–216.
62. Assmy P, et al. (2013) Thick-shelled, grazer-protected diatoms decouple ocean carbon and silicon cycles in the iron-limited Antarctic circumpolar current. *Proc Natl Acad Sci USA* 110:20633–20638.
63. Birol I, et al. (2009) De novo transcriptome assembly with ABySS. *Bioinformatics* 25:2872–2877.
64. Kanehisa M, Furumichi M, Tanabe M, Sato Y, Morishima K (2017) KEGG: New perspectives on genomes, pathways, diseases and drugs. *Nucleic Acids Res* 45:D353–D361.
65. Keeling PJ, et al. (2014) The marine microbial eukaryote transcriptome sequencing project (MMETSP): Illuminating the functional diversity of eukaryotic life in the oceans through transcriptome sequencing. *PLoS Biol* 12:e1001889.
66. Patro R, Duggal G, Love MI, Irizarry RA, Kingsford C (2017) Salmon provides fast and bias-aware quantification of transcript expression. *Nat Methods* 14:417–419.
67. Love MI, Huber W, Anders S (2014) Moderated estimation of fold change and dispersion for RNA-seq data with DESeq2. *Genome Biol* 15:550.
68. Twining BS, et al. (2011) Metal quotas of plankton in the equatorial Pacific Ocean. *Deep Sea Res Pt II* 58:325–341.
69. Nunez-Milland DR, Baines SB, Vogt S, Twining BS (2010) Quantification of phosphorus in single cells using synchrotron x-ray fluorescence. *J Synchrotron Radiat* 17: 560–566.
70. Twining BS, Baines SB, Fisher NS, Landry MR (2004) Cellular iron contents of plankton during the Southern Ocean iron experiment (SOFeX). *Deep Sea Res Pt I* 51:1827–1850.
71. Cohen NR, Lampe RH, Marchetti A (2016) Metatranscriptomics of eukaryotic phytoplankton incubations for iron storage study in the California Upwelling Zone Raw sequence reads. Sequence Read Archive. Available at https://www.ncbi.nlm.nih.gov/sra/SRP074302. Deposited July 21, 2016.
72. Cohen NR, Lampe RH, Marchetti A (2018) Uncultured eukaryotic phytoplankton raw sequence reads. Sequence Read Archive. Available at https://www.ncbi.nlm.nih.gov/sra/SRP108216. Deposited May 29, 2017.
73. Boyer TP, et al. (2013) World Ocean Database 2013, *NOAA Atlas NESDIS 72*, Eds Levitus S, Mishonov A (NODC, Silver Spring, MD).